COMPARING MODEL SIMULATIONS OF THREE BENCHMARK TSUNAMI GENERATION CASES

By Philip Watts[1], Fumihiko Imamura[2] and Stéphan Grilli[3]

[1]Applied Fluids Engineering, PMB #237, 5710 E. 7th Street, Long Beach, CA 90803.
[2]Prof., Disaster Control Research Center, School of Engrg., Tohoku University, Aoba 06, Sendai 980-8579, Japan.
[3]Prof., Dept. Ocean Engineering, University of Rhode Island, Narragansett, RI 02882.

KEYWORDS: Tsunami, tidal wave, wave generation, benchmark case, simulation, underwater landslide, submarine landslide, sub-aqueous landslide

ABSTRACT: Three benchmark cases are proposed to study tsunamis generated by underwater landslides. Two distinct numerical models are applied to each benchmark case. Each model involves distinct center of mass motions and rates of landslide deformation. Computed tsunami amplitudes agree reasonably well for both models, although there are differences that remain to be explained. One of the benchmark cases is compared to laboratory experiments. The agreement is quite good with the models. Other researchers are encouraged to employ these benchmark cases, in future experimental or numerical work.

INTRODUCTION

Tsunamis generated by underwater landslides are receiving more attention following analyses demonstrating that the surprisingly large local tsunami documented during the 1998 Papua New Guinea catastrophe was generated by submarine mass failure (Kawata *et al.*, 1999; Tappin *et al.*, 1999, 2000; Synolakis *et al.*, 2000). In response to these and other studies, recent work by marine geologists now considers the tsunamigenic potential of submarine mass failure scars (Goldfinger *et al.*, 2000; Driscoll *et al.*, 2000). Despite these advances in the observational science, there remains no validation of the numerical models currently in use. Consequently, the ability of scientists to simulate tsunami generation by underwater landslides remains in doubt. Note, underwater landslides are also called submarine mass failures and display a wide range of morphological features (Prior and Coleman, 1979; Edgers and Karlsrud, 1982; Hampton *et al.*, 1996).

Researchers have tackled tsunami generation by underwater landslides with a wide variety of numerical methods incorporating many different assumptions. Iwasaki (1987, 1997) and Verriere and Lenoir (1992) utilized linear potential theory to simulate wave generation by moving the domain boundary. Depth-averaged Nonlinear Shallow Water (NSW) wave equations were solved by Fine *et al.* (1998), Harbitz (1992), Imamura and Gica (1996), and Jiang and LeBlond (1992, 1993, 1994), in combination with disparate landslide models. Fully nonlinear fluid dynamic field equations were solved by Assier Rzadkiewicz *et al.* (1997), Grilli and Watts (1999) (in an irrotational and inviscid approximation), and Heinrich (1992), in concert with assorted landslide models. Watts *et al.* (2000) appears to be the only work to compare tsunami generation for different center of mass motions and different rates of landslide deformation. For the most part, scientists have studied vastly different landslide geometries, motions, and constitutive behaviors. There is currently no consensus on the ability of these different models to reproduce tsunami generation by underwater landslides.

To further advance research in tsunami generation by underwater landslides, benchmark cases are needed to validate numerical models and to help explain the origins of any discrepancies that may exist, both between numerical models, and with comparisons to experimental results. Benchmark problems are already available for tsunami propagation and inundation (Liu *et al.*, 1991; Yeh *et al.*, 1996). Our goal in this work is to establish three benchmark cases for future reference by researchers interested in tsunami generation by underwater landslides, and to compare simulations, for one of these cases, to recently performed laboratory experiments. Each case is two-dimensional in order to reduce computational or experimental effort.

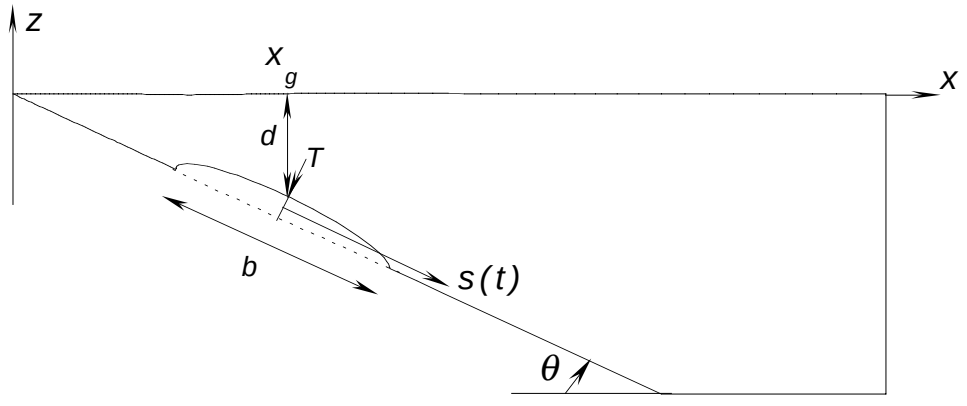

Figure 1: Definition sketch of the simulation domain in II and GW Models, and of initial landslide parameters

We compare results from two distinct numerical models. We hope that this work will promote future numerical and experimental comparisons. The comparisons made here are by no means the end of this effort.

BENCHMARK CASES

To facilitate their experimental realization, the benchmark cases chosen for this work are based in part on the sliding block experiments of previous researchers (Heinrich, 1992; Iwasaki, 1982; Watts, 1997; Wiegel, 1955). A straight incline forms a planar beach with the coordinate origin at the undisturbed beach and the positive x-axis oriented horizontally away from the shoreline (Fig. 1). A semi-ellipse approximates the initial landslide geometry. Landslide deformation is permitted following incipient motion of the semi-ellipse. The nominal underwater landslide length measured along the incline is b =1000 m for all three cases. All underwater landslides are assumed to have a bulk density ρ_b =1900 kg/m^3 and fail in sea water of density ρ_o =1030 kg/m^3. The geometrical parameters for each benchmark case are given in Table 1. The initial submergence at the middle of the landslide, $x = x_g$, was obtained from a scaled reference equation $d = b \sin\theta$, while the initial landslide thickness was calculated from another scaled reference equation, $T = 0.2\ b \sin\theta$ (Watts *et al.*, 2000). A wave gage was situated above the middle of the initial landslide position at $x_g = (d + T/\cos\theta)/\tan\theta$, and recorded tsunami elevation $\eta(t)$. Dimensional quantities are presented throughout since different numerical techniques employ different non-dimensional schemes. Watts (1998) provides the correct Froude scaling to perform these benchmark experiments at laboratory scale.

Table 1: Underwater landslide and numerical wave gage parameters for benchmark cases c_1, c_2, and c_3

Case (1)	θ (2)	b (m) (3)	T (m) (4)	d (m) (5)	x_g (m) (6)
c_1	30˚	1000	100	500	1066
c_2	15˚	1000	51.8	259	1166
c_3	5˚	1000	17.4	87.2	1196

LABORATORY EXPERIMENTS

Laboratory experiments were conducted in the University of Rhode Island wavetank (length 30 m, width 3.6 m, depth 1.8 m). This tank is equipped with a modular beach made of 8 independently adjustable panels (3.6 m by 2.4 m) whose difference in slope can be up to 15°. Benchmark case 2 was tested in the wave tank at 1:1000 scale, in the set-up shown in Fig. 2. Two beach panels were set to an angle θ =15° and covered by a smooth aluminium plate. A quasi two-dimensional experiment was realized by building vertical (plywood) side walls at a small distance (about 15 cm) from each other. A semi-elliptical wood and plastic landslide model was built and installed in between the walls. The model was equipped with low-friction wheels and a lead ballast was added to achieve the correct bulk density (Fig. 3). An accelerometer was attached to the model center of gravity to measure landslide kinematics. Four capacitance wave gages were mounted on an overhead carriage, to measure free surface elevation (Fig. 2), the first gage being located at $x = x_g$ and the others mounted 30 cm apart with increasing x-positions.

Figure 2: Quasi two-dimensional landslide experiments for benchmark case 2

Figure 3: Close-up of scale model for two-dimensional landslide experiments

Experiments were repeated at least five times and the repeatability of results was very good. Results are presented in a following section.

NUMERICAL MODEL DESCRIPTIONS

Imamura and Imteaz (1995) developed a mathematical model for a two-layer flow along a non-horizontal bottom. Conservation of mass and momentum equations were depth-integrated in each layer, and nonlinear kinematic and dynamic conditions were specified at the free surface and at the interface between fluids. Both fluids had uniform densities and were immiscible. Vertical velocity distributions were assumed within each fluid layer. The landslide fluid was ascribed a uniform viscosity, which sensitivity analyses show has very little effect on wave records over a range of viscosities 1-100 times that of water. A staggered leap-frog finite difference scheme, with a second-order truncation error was used to solve the governing equations. Landslides were thus modeled as immiscible fluid flows comprising a second layer, as in the work of Jiang and LeBlond (1992, 1993, 1994). An instantaneous local force balance governed landslide motion. Hence, this motion resulted from the solution of the problem itself and was not externally specified as a boundary condition. We will refer to this numerical model as the II Model below.

Grilli *et al.* (1989, 1996) developed and validated a two-dimensional Boundary Element Model (BEM) of inviscid, irrotational free surface flows (i.e., potential flow theory). Cubic boundary elements were used for the discretization of boundary geometry, combined with fully nonlinear boundary conditions and second-order accurate time updating of free surface position. The model was experimentally validated for long wave propagation and runup or breaking over slopes by Grilli *et al.* (1994, 1998). Model predictions are

surprisingly accurate; for instance, the maximum discrepancy for solitary waves shoaling over slopes is 2% at the breaking point, between computed and measured wave shapes. Grilli and Watts (1999) applied this BEM model to water wave generation by underwater landslides and performed a sensitivity analysis for one underwater landslide scenario. The landslide center of mass motion along the incline was prescribed by the analytical solutions of Watts (1998, 2000) (see next section). In these computations, the landslide retained its semi-elliptic shape while translating along the incline. We will refer to this numerical model as the GW Model below.

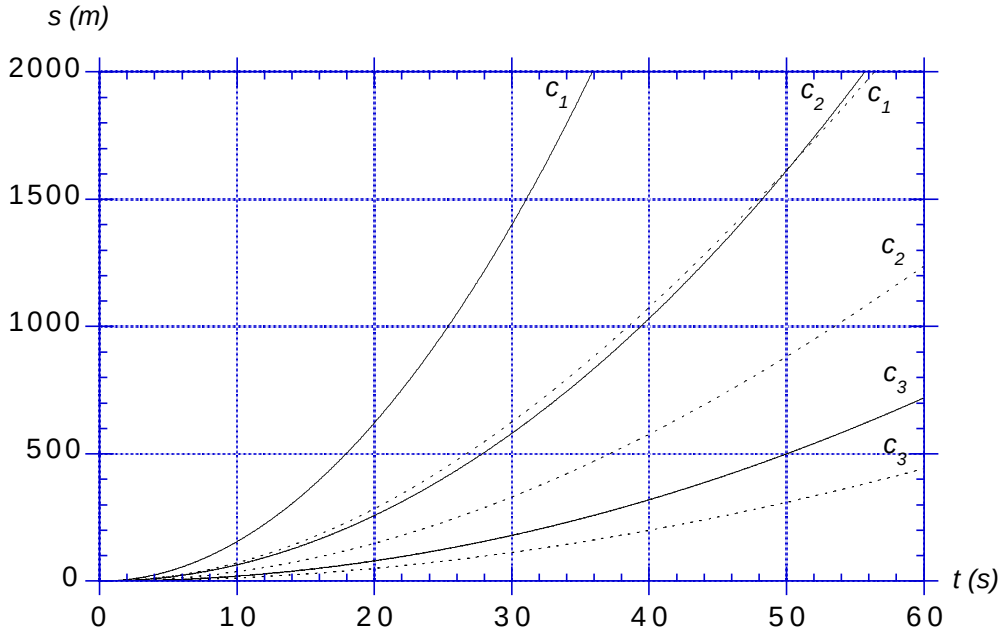

Figure 4: Underwater landslide center of mass motion as a function of time in the II (solid) and GW (dashed) Models, for benchmark cases c_1, c_2, and c_3 in Table 2

Both the II and GW Models are used in the following to simulate tsunamis generated by underwater landslides of identical initial characteristics corresponding to the three benchmark cases in Table 1. For discretization techniques and numerical parameters used in both models, please refer to Imamuraand Imteaz (1995) and Grilli and Watts (1999).

SIMULATION RESULTS

Descriptions of tsunami generationby underwater landslides should begin by documenting landslide center of mass motion and rates of deformation. Since both motion and deformation were prescribed in the GWModel, we proceed to describe the results obtained

from the II Model and compare these results with the GW Model. We also relate the measured initial acceleration obtained for case 2. Assuming the center of mass motion *s(t)* is parallel to the incline (Fig. 1), Fig. 4 shows the center of mass motions obtained in the II Model for the three benchmark cases. It is readily verified that the simple equation

$$s(t) = \frac{a_o\, t^2}{2} \tag{1}$$

provides an accurate fit of these motions. Eq. (1) is the first term in a Taylor series expansion of landslide motion beginning at rest (Watts, 2000). In fact, two-parameter curve fits of the equation of motion given in Watts (1998) (and reproduced as Eq. (3) below) failed to produce unique parameter values, due to the accuracy of the one-parameter fit given by Eq. (1). Two curve fitting parameters introduced a redundancy in the solution algorithm that yielded infinite fitted solutions. Values of initial landslide accelerations a_o for the II Model obtained by curve fitting Eq. (1) can be found in Table 2. Note that R^2 coefficients were 0.99 or better for all of the fits. The experimental initial acceleration was a_o = 0.73 m/s^2 for case 2. This compares favorably with the value from the GW Model in Table 2 and suggests an added mass coefficient $C_m \approx 1.2$ given negligible rolling friction.

Table 2: Initial accelerations, terminal velocity and rates of deformation in II and GW Models

Case	a_{oII} (m/s^2)	a_{oGW} (m/s^2)	u_{tGW} (m/s)	Γ_{II} (s^{-1})	Γ_{GW} (s^{-1})
(1)	(2)	(3)	(4)	(5)	(6)
c_1	3.11	1.47	80.9	0.062	0.000
c_2	1.29	0.76	57.8	0.035	0.000
c_3	0.40	0.26	33.2	0.017	0.000

Landslide deformation in the II Model was manifested foremost as an extension in time, *b(t)*, of the initial landslide length b_o. Fig. 5 demonstrates that the non-dimensional ratio b/b_o varies almost linearly with time, following an initial transient, similar to the experimental observations made by Watts (1997) for a submerged granular mass. A semi-empirical expression that describes landslide extension is

$$b(t) = b_o \{1 + \Gamma t \ [1 - \exp(-K t)]\} \qquad (2)$$

where Γ is the eventual linear rate of extension and the exponential term describes an initial transient, with $K = a_o / g\Gamma$ (Watts *et al.*, 2000). The parameter K is chosen to fix the uppermost landslide corner in place as the center of mass begins to accelerate. Table 2 gives values of Γ for the II Model found from curve fits of Eq. (2).

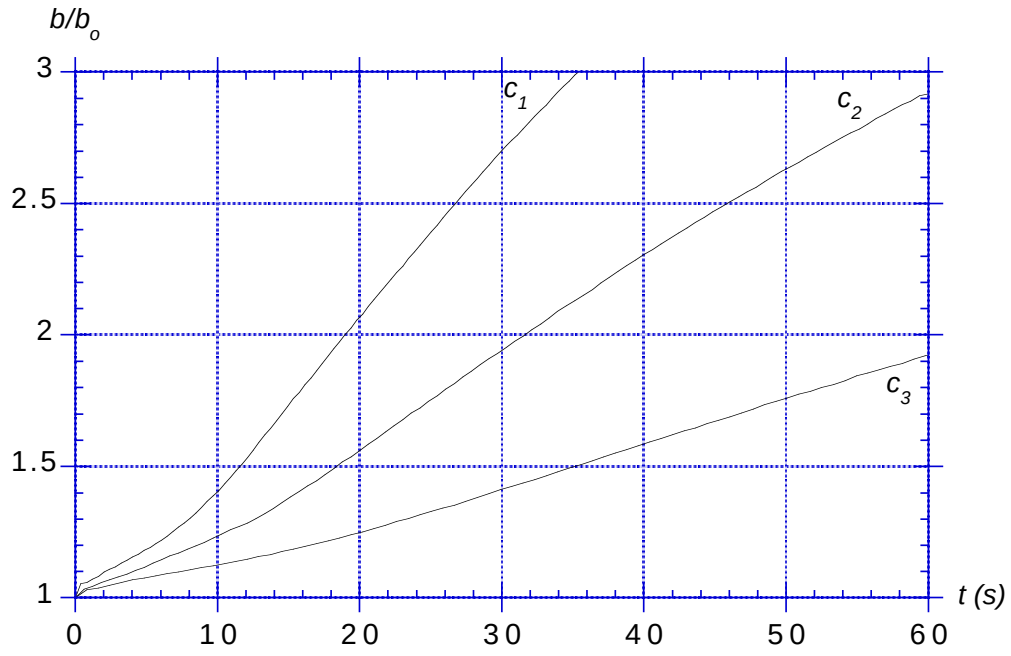

Figure 5: Underwater landslide temporal extension in II Model

Watts (1998) developed a wavemaker formalism for non-deforming underwater landslides, based on an analytical solution of center of mass motion

$$s(t) = s_o \ln \left[\cosh \left(\frac{t}{t_o} \right) \right] \qquad (3)$$

with

$$s_o = \frac{u_t^2}{a_o} \quad , \quad t_o = \frac{u_t}{a_o} \qquad (4a,b)$$

where a_o and u_t denote landslide initial acceleration and terminal velocity, respectively (see Eq. (5) and discussion in the following section). Eqs. (3) and (4) were used in the GW Model to specify the landslide kinematics. Eq. (4) can also be expressed as a function of

the landslide physical parameters: initial length, incline angle, and density (Watts, 1998). For the three benchmark cases, using the data in Table 1, we find the values of a_o and u_t

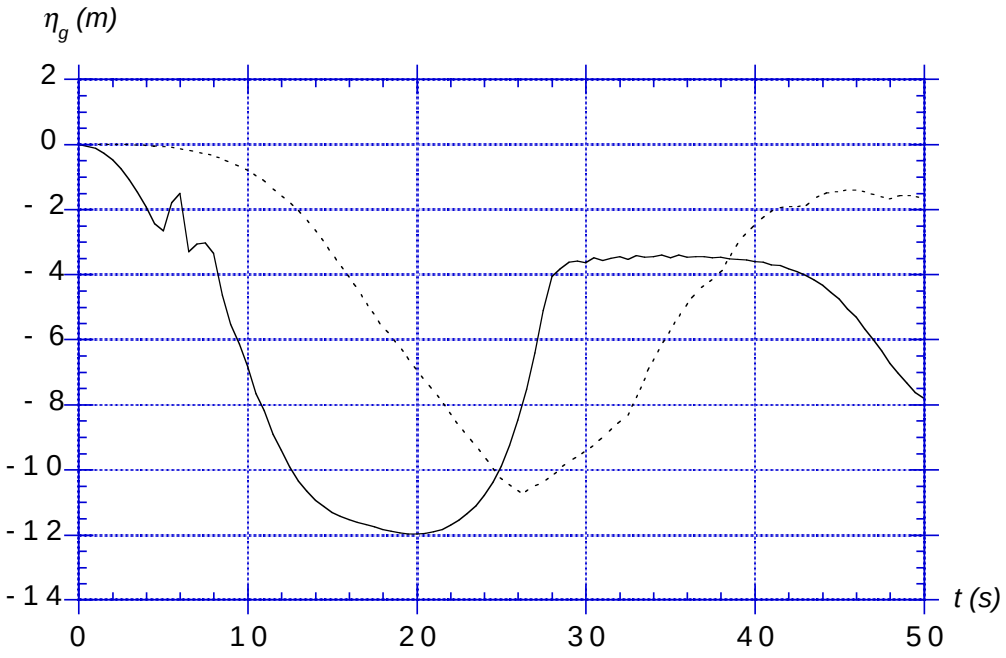

Figure 6: Numerical wave gage record at x_g = 1066 m for benchmark case 1; II Model (solid); GW Model (dashed)

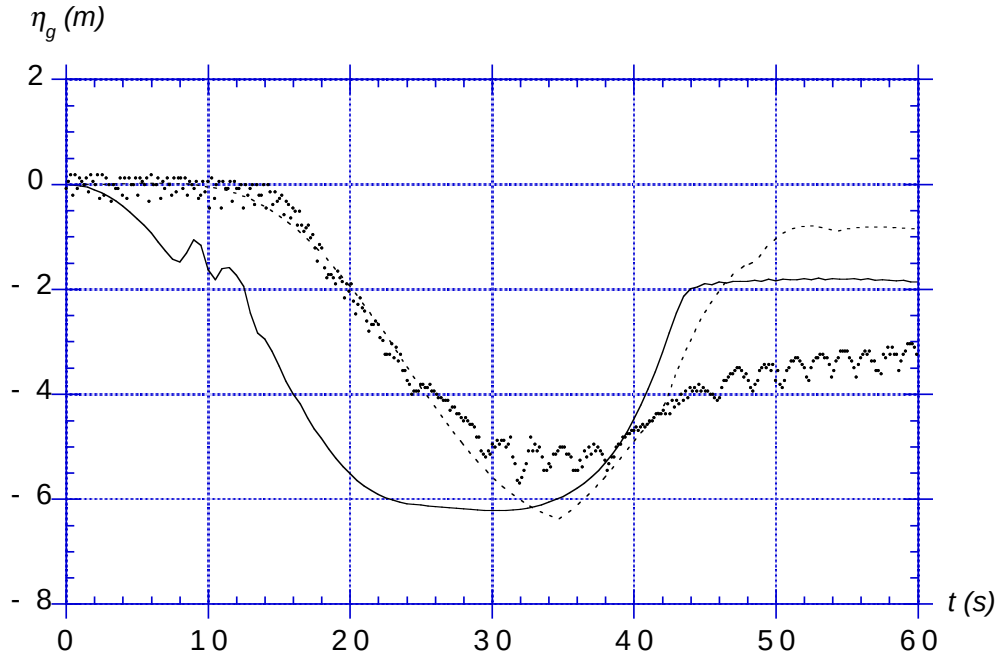

Figure 7: Numerical wave gage record at x_g = 1166 m for benchmark case 2; II Model (solid); GW Model (dashed); scaled-up experiments (dots)

listed in Table 2 and corresponding motion *s(t)* shown in Fig. 4. Note, as discussed above, no extension Γ was specified in the GW Model.

Figures 6-8 show the tsunami simulation results of both numerical models for cases 1-3, respectively. The GW and II Model results agree qualitatively for all three cases, although the GW Model produces slightly smaller wave amplitudes. The II Model produces more acute free surface curvature near t = 0 as well as longer tsunami periods. Maximum tsunami amplitudes at the numerical wave gages are given in Table 3. This is the same characteristic tsunami amplitude employed in the scaling analyses of Watts (1998, 2000). Note, the II Model has water wave disturbances in the first 5-20 s of each simulation brought on by a Kelvin-Helmholtz type instability along the landslide-water interface.

Table 3: Simulated and calculated characteristic wave amplitudes

Case (1)	η_{II} (m) (2)	η_{GW} (m) (3)	η_{PP} (m) (4)
c_1	11.98	10.86	15.71
c_2	6.22	6.37	8.14
c_3	2.07	2.39	2.73

DISCUSSION

Tsunami generation in the shallow water wave limit occurs through vertical acceleration of some region on the ocean floor (Tuck and Hwang, 1972; Watts *et al.*, 2000). Since the center of mass motion modeled in the II Model, as shown in Fig. 4, corresponds to the landslide acceleration described by Eq. (1), tsunami generation by the II Model in Figs. 6-8 can be directly associated with vertical landslide acceleration. Tsunami generation in a potential flow model such as the GW Model, however, occurs through gradients of the velocity potential at the free surface, which can arise from both horizontal and vertical landslide motions. Also, tsunami generation in the GW Model is theoretically not limited to landslide acceleration and may include the instantaneous water velocity distribution.

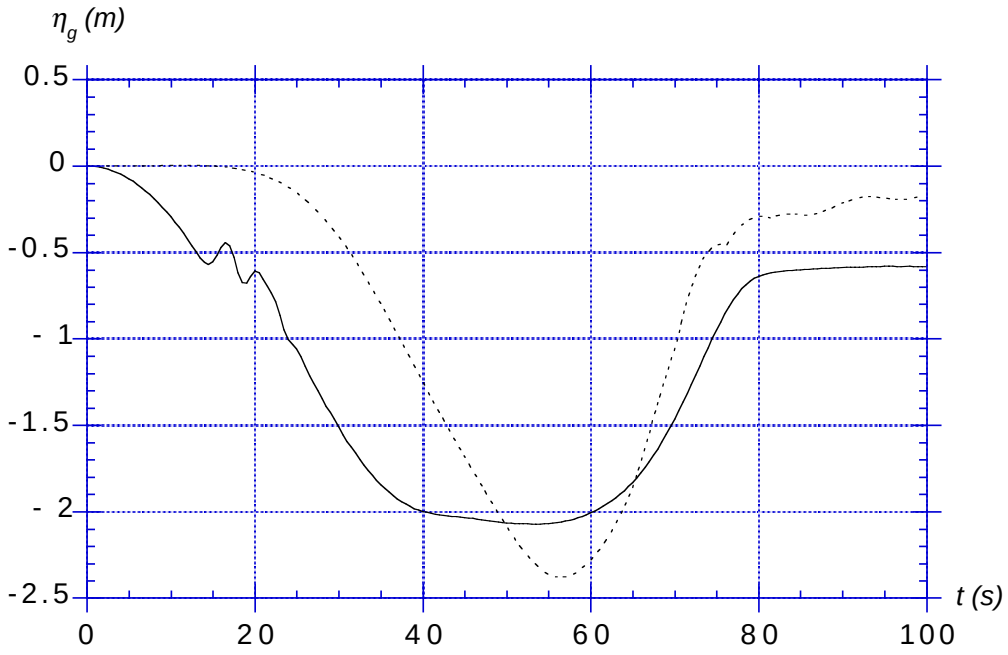

Figure 8: Numerical wave gage record at x_g = 1196 m for benchmark case 3; II Model (solid); GW Model (dashed)

The initial center of mass motion during landslide tsunami generation can be accurately described by Eq. (1), assuming the correct initial acceleration is known. Along an infinite incline, an equation such as (3) provides a better description of the motion. Watts (1998) provides an analytical method for choosing between Eqs. (1) and (3) based on the length of the incline.

Tsunami amplitude is scaled by the landslide initial acceleration (Watts, 1998, 2000). The initial accelerations listed in Table 2 differ considerably between the two models, despite identical initial landslide shapes and bulk densities. The theoretical initial acceleration specified in the GW Model is, neglecting Coulomb friction,

$$\frac{a_o}{g} = \frac{(\gamma - 1)\sin\theta}{\gamma + C_m} \tag{5}$$

in which γ represents the landslide specific density and C_m an added mass coefficient. Eq. (5) applies specifically to underwater landslides that experience negligible basal friction due to phenomena such as water injection or liquefaction (Watts *et al.*, 2000). The value C_m = 1 used in the GW Model produces conservative landslide motions. Our experimental

results suggest that $C_m = 1$ is a reasonable estimate of the actual added mass coefficient. If $C_m \approx 0$ were a better approximation for underwater landslide motion, then the GW Model initial accelerations listed in Table 2 would increase by about 50%, and would agree better with those of the II Model. A vanishing added mass coefficient may be more representative of the initial accelerations found from a depth-averaged model. Indeed, the initial acceleration found in the II Model for case 3 agrees well with Eq. (5), if $C_m \approx 0$. This is the least inclined slope studied. However, the initial accelerations found in the II Model for cases 1 and 2, which have larger incline angles, were larger than the corresponding maximal values from Eq. (5) with $C_m \approx 0$. This contradicts Eq. (5), which was derived for rigid body motion.

The additional center of mass acceleration in the II Model can be explained by landslide deformation. Landslide deformation shifts mass forward (during formation of a landslide nose) and results in an advance of the center of mass. The rapid shift in center of mass experienced in the II Model may arise from model assumptions that are not present in actual underwater landslides. The rates of landslide extension reported in Table 2, for the II Model, are 3-6 times greater than the maximum rate

$$\Gamma_{\max} \approx \frac{\sqrt{\sin\theta}}{6}\sqrt{\frac{g}{b_o}} \tag{6}$$

estimated by Watts *et al.* (2000). These large rates of extension may arise from the assumption that the landslide behaves like an immiscible, homogeneous fluid with relatively low viscosity. A non-deforming landslide has infinite viscosity. For rates of extension given by Eq. (6), Watts *et al.* (2000) show that there is very modest change in the shape of the wave gage record. One such change is an increase of the curvature around $t = 0$, similar to the results from the II Model. The additional curvature shown in Figs. 6-8 can therefore be ascribed to landslide deformation.

We also note that the experimental work of Watts (1997) showed diminished wave amplitudes from deforming underwater landslides. This was an experimental artifact produced by flow through the granular media used to reproduce a landslide at laboratory scale. Watts *et al.* (2000), however, showed very small changes in characteristic wave amplitude with the GW Model when using rates of extension given by Eq. (6). Characteristic wave amplitudes were either increased or decreased depending on the incline

angle. This suggests a complex relationship between landslide extension and tsunami amplitude.

A characteristic tsunami amplitude can form the basis of wavemaker curves and provide a valuable tsunami scaling quantity (Watts, 1998, 2000). The characteristic tsunami amplitude chosen here is the maximum depression measured by the wave gages in Figs. 6-8. Table 3 summarizes the characteristic tsunami amplitudes obtained for each benchmark case. Tsunami amplitudes from the two models differ by –10% to +13%, as the incline angle decreases. These amplitudes compare favorably with the analytical prediction of Pelinovsky and Poplavsky (1996) for the same landslide parameters, denoted by PP in Table 3. While discrepancies remain, there is general agreement over the characteristic tsunami amplitudes.

Larger initial accelerations produce larger tsunami amplitudes. The change in characteristic amplitude can be quantified by choosing an effective landslide density. We calculate the expected increase in wave amplitude for the II Model by calculating an effective specific density from Eq. (5) (with C_m = 1), using the observed center of mass acceleration produced by the II Model (Table 2). For case 2, for instance, the specific density $\gamma = 3.07$ reproduces an equivalent center of mass motion, using Eqs. (1) and (5), to that measured for the II Model. We now employ curve fits of characteristic amplitude versus specific density given by Watts *et al.* (2000) to scale the tsunami amplitude. We find a factor of 1.6 increase in wave amplitude for case 2 due to the increase in effective landslide density. This correction is made possible by a rigorous analysis of landslide motion. Hence, if the II Model had reproduced an initial acceleration equal to that of the GW Model for case 2, then we would expect the wave record shown in Fig. 7 to be 1.6 times smaller. Repeating this correction for all of the benchmark cases, we would find that wave records from the II Model would become smaller than wave records from the GW Model. Once the characteristic amplitude is corrected for the different initial accelerations, the remaining differences in characteristic amplitude between the two models are primarily due to depth averaging and landslide deformation. Hence, in view of these results, we conclude that depth averaging of the equations in the II Model leads to reduced tsunami amplitudes.

We repeat here model differences that could account for the results in Figs. 6-8. The GW Model solves a full set of fluid dynamic equations whereas the II Model depth-averages the flow in each fluid layer. The GW Model prescribes center of mass motion with Eqs. (3) to (5) and does not simulate landslide deformation. The II Model allows the landslide fluid to

deform while undergoing motion derived from a local force balance. Qualitative differences in tsunami generation may be drawn from the comparisons made herein. Tsunami amplitudes, once corrected to match initial accelerations, may be larger in the GW Model due to the combined influences of both horizontal acceleration and landslide velocity on wave generation. If this is true, then the effective density of the II Model increases tsunami amplitude, while depth averaging decreases tsunami amplitude. The net effect leads to reasonable agreement between the two models. The general agreement in tsunami amplitude between the two models should probably be viewed as an outcome of some mean value theorem: the large number of mechanically plausible assumptions built into each model tends to produce similar outputs. More controlled comparisons of model results, however, are required in the future. Finally, a consequence of this work is that landslide tsunami generation, made with numerical models based on the seminal work of Jiang and Leblond (1992, 1993, 1994), i.e., using depth-averaged NSW equations, appears to have the potential to consistently underpredict tsunami amplitude, if rates of landslide deformation are not large.

CONCLUSIONS

Three benchmark cases for tsunamis generated by underwater landslides are proposed in this paper. These benchmark cases are considerably tsunamigenic and reinforce the significant hazard of tsunami generation by submarine mass failure in general. The underwater landslide initial acceleration and rate of deformation are both needed to compare benchmark simulations or experiments. Underwater landslide center of mass motion during tsunami generation can be described by the initial acceleration in Eqs. (1) and (5) whenever rates of landslide extension are less than values indicated by Eq. (4). Experimental results and numerical simulations to date indicate that the primary mode of landslide deformation consists of a linear rate of extension. Larger initial accelerations produce larger tsunami amplitudes. The characteristic tsunami amplitudes differed by up to 13% for the two numerical models compared here. Experimental results available for benchmark case 2 showed a better agreement with the GW Model results, in part because landslide deformation changes the shape of the wave gage record. Depth-averaged tsunami generation appears to underpredict tsunami amplitude. Further interpretation of existing model differences awaits more detailed model comparisons. We have endeavored to begin a process of comparing numerical simulations and experimental realizations for three benchmark cases. We hope the process will continue.

ACKNOWLEDGEMENTS

This work arose from a discussion at the 1999 IUGG General Meeting in Birmingham, U. K. at which time all tsunami scientists were invited to participate in landslide tsunami benchmark simulations. The authors are grateful for support from Applied Fluids Engineering, Inc. and the Disaster Control Research Center at Tohoku University.

REFERENCES

Assier Rzadkiewicz, S., Mariotti, C., and Heinrich, P. (1997). "Numerical simulation of submarine landslides and their hydraulic effects." *J. Wtrwy, Port, Coast, and Oc. Engrg.*, ASCE, 123(4), 149-157.

Driscoll, N. W., Weissel, J. K., Goff, J. A. (2000). "Potential for large-scale submarine slope failure and tsunami generation along the U.S. Mid-Atlantic Coast." *Geology*, in press.

Edgers, L., and Karlsrud, K. (1982). "Soil flows generated by submarine slides: Case studies and consequences." *Nor. Geotech. Inst. Bull.*, 143, 1-11.

Fine, I. V., Rabinovich, A. B., Kulikov, E. A., Thomson, R. E., and Bornhold, B. D. (1998). "Numerical modelling of landslide-generated tsunamis with application to the Skagway Harbor tsunami of November 3, 1994." *Proc. Tsunami Symp.*, Paris.

Goldfinger, C., Kulm, L. D., McNeill, L. C., Watts, P. (2000). "Super-scale failure of the Southern Oregon Cascadia Margin." *PAGEOPH*, 157, 1189-1226.

Grilli, S. T., Skourup, J., and Svendsen, I. A. (1989). "An efficient boundary element method for nonlinear water waves." *Engrg. Analysis with Boundary Elements*, 6(2), 97-107.

Grilli, S. T., Subramanya, R., Svendsen, I. A. and Veeramony, J. (1994) Shoaling of Solitary Waves on Plane Beaches. ." *J. Wtrwy, Port, Coast, and Oc. Engrg.*, ASCE, 120(6), 609-628.

Grilli, S. T., and Subramanya, R. (1996). "Numerical modeling of wave breaking induced by fixed or moving boundaries." *Comp. Mech.*, 17, 374-391.

Grilli, S. T., Svendsen, I. A., and Subramanya, R. (1998). "Breaking criterion and characteristics for solitary waves on slopes -- Closure." *J. Wtrwy, Port, Coast, and Oc. Engrg.*, ASCE, 124(6), 333-335.

Grilli, S. T., and Watts, P. (1999). "Modeling of waves generated by a moving submerged body: Applications to underwater landslides." *Engrg. Analysis with Boundary Elements*, 23(8), 645-656.

Hampton, M. A., Lee, H. J., and Locat, J. (1996). "Submarine landslides." *Rev. Geophys.*, 34(1), 33-59.

Harbitz, C. B. (1992). "Model simulations of tsunamis generated by the Storegga slides." *Marine Geology*, 105, 1-21.

Heinrich, P. (1992). "Nonlinear water waves generated by submarine and aerial landslides." *J. Wtrwy, Port, Coast, and Oc. Engrg.*, ASCE, 118(3), 249-266.

Imamura, F., and Imteaz, M. M. A. (1995). "Long waves in two-layers: Governing equations and numerical model." *J. Sci. Tsunami Hazards*, 13, 3-24.

Imamura, F., and Gica, E. C. (1996). "Numerical model for tsunami generation due to subaqueous landslide along a coast." *Sci. Tsunami Hazards*, 14, 13-28.

Iwasaki, S. (1982). "Experimental study of a tsunami generated by a horizontal motion of a sloping bottom." *Bull. Earth. Res. Inst.*, 57, 239-262.

Iwasaki, S. (1987). "On the estimation of a tsunami generated by a submarine landslide." *Proc., Int. Tsunami Symp.*, Vancouver, B.C., 134-138.

Iwasaki, S. (1997). "The wave forms and directivity of a tsunami generated by an earthquake and a landslide." *Sci. Tsunami Hazards*, 15, 23-40.

Jiang, L., and LeBlond, P. H. (1992). "The coupling of a submarine slide and the surface waves which it generates." *J. Geoph. Res.*, 97(C8), 12731-12744.

Jiang, L., and LeBlond, P. H. (1993). "Numerical modeling of an underwater Bingham plastic mudslide and the waves which it generates." *J. Geoph. Res.*, 98(C6), 10303-10317.

Jiang, L., and LeBlond, P. H. (1994). "Three-dimensional modeling of tsunami generation due to a submarine mudslide." *J. Phys. Ocean.*, 24, 559-573.

Kawata, Y. and International Tsunami Survey Team members. (1999). "Tsunami in papua New guinea was intense as first thought." *Eos, Trans. Am. Geophys. Union*, 80(9), 101.

Liu, P.L.-F., Synolakis, C. E., Yeh, H. H. (1991). "Tsunami in Papua New Guinea was intense as first thought." *J. Fluid Mech.*, 229, 675-688.

Synolakis, C. E., Bardet, J.-P., Borrero, J. C., Davies, H., Grilli, S. T., Okal, E. A., Silver, E., Sweet, S., Tappin, D. R., Watts, P. The Slump Origin of the 1998 Papua New Guinea Tsunami. *Proc. Royal Society*, A (submitted).

Pelinovsky, E., and Poplavsky, A. (1996). "Simplified model of tsunami generation by submarine landslide." *Phys. Chem. Earth*, 21(12), 13-17.

Prior, D. B., and Coleman, J. M. (1979). "Submarine landslides: Geometry and nomenclature." *Z. Geomorph. N. F.*, 23(4), 415-426.

Tappin, D. R. , Matsumoto, T., and shipboard scientists. (1999). "Offshore surveys identify sediment slump as likely cause of devastating Papua New Guinea tsunami 1998.", *Eos, Trans. Am. Geophys. Union*, 80(30), 329.

Tappin, D. R., Watts, P., McMurtry, G. M., Lafoy, Y., Matsumoto, T. (2000). "The Sissano Papua New Guinea tsunami of July 1998 – Offshore evidence on the source mechanism.", *Marine Geol*. (in press).

Tuck, E. O., and Hwang, L.-S. (1972). "Long Wave Generation on a Sloping Beach." *J. Fluid Mech.*, 51(3), 449-461.

Verriere, M., and Lenoir, M. (1992). "Computation of waves generated by submarine landslides." *Int. J. Num. Methods Fluids*, 14, 403-421.

Watts, P. (1997). "Water waves generated by underwater landslides," PhD thesis, California Inst. of Technol., Pasadena, CA.

Watts, P. (1998). "Wavemaker curves for tsunamis generated by underwater landslides." *J. Wtrwy, Port, Coast, and Oc. Engrg.*, ASCE, 124(3), 127-137.

Watts, P. (2000). "Tsunami features of solid block underwater landslides." *J. Wtrwy, Port, Coast, and Oc. Engrg.*, ASCE, 126(3), 144-152.

Watts, P., Grilli, S. T., and Synolakis, C. E. (2000). "Tsunami generation by submarine mass failure. I: Wavemaker models." *J. Wtrwy, Port, Coast, and Oc. Engrg.*, ASCE (submitted).

Wiegel, R. L. (1955). "Laboratory studies of gravity waves generated by the movement of a submarine body." *Trans. Am. Geophys. Union*, 36(5), 759-774.

Yeh, H. H., Liu, P.L.-F., Synolakis, C. E. (1996). *Long-wave runup models: Friday Harbor, USA, 12-17 Sept. 1995*. World Scientific, Singapore.